Scientific Research Publishing

Journal of Power and Energy Engineering, 2025, 13(9), 186-206
https://www.scirp.org/journal/jpee
ISSN Online: 2327-5901
ISSN Print: 2327-588X

Optimization of Free-Flow Water Turbine of Pico-Hydropower Using Computational Fluid Dynamic Analysis

Nurul Ashikin Mohd Rais[1], Adib Zikry Abdul Kasimin[1], Mohd Ikram Mohd Nor Rizan[2]

[1]Faculty of Technology and Electrical Engineering, Universiti Teknikal Malaysia Melaka, Melaka, Malaysia
[2]Academy of Language Studies, Universiti Teknologi MARA Kampus Seremban, Negeri Sembilan, Malaysia
Email: nurulashikin@utem.edu.my

How to cite this paper: Rais, N.A.M., Kasimin, A.Z.A. and Rizan, M.I.M.N. (2025) Optimization of Free-Flow Water Turbine of Pico-Hydropower Using Computational Fluid Dynamic Analysis. *Journal of Power and Energy Engineering*, **13**, 186-206.
https://doi.org/10.4236/jpee.2025.139013

Received: August 10, 2025
Accepted: September 19, 2025
Published: September 22, 2025

Abstract

The increasing global demand for sustainable energy solutions has driven research into pico-hydropower systems as an efficient and environmentally friendly method for harnessing renewable energy. This study focuses on the optimization of free-flow water turbine applications using Computational Fluid Dynamics (CFD) analysis. Free-flow turbines, which operate in rivers or channels without the need for large-scale infrastructure, offer significant advantages in terms of cost, ecological impact, and ease of deployment. The research employs advanced CFD techniques to evaluate and enhance the performance of a turbine under various conditions. Key design parameters, including water flow rates of 2 L/s, water heads of less 5 m, turbine diameters of 0.75 m and 1 m, nozzle sizes at 10 mm, 12 mm and 15 mm and the pipe diameters setting of 0.75 inch and 1 inch. Optimization algorithms are integrated with CFD simulations to identify the most efficient configurations. The findings reveal the critical role of hydrodynamic optimization in improving the energy conversion efficiency of pico-hydropower turbines. The results identified the 1 m turbine with 0.75 inch pipe size at 12 mm nozzle diameter give the optimal design, achieving a maximum power out at 100 W with 5 m and 3 m water head. The optimized turbine design demonstrated a significant improvement in performance compared to existing models, validating the potential of CFD as a powerful tool for innovation in hydropower technology.

Keywords

Free-Flow, Water Turbine, Water Head, Pico-Hydropower, CFD

1. Introduction

The global transition toward renewable energy is accelerating as societies strive to address environmental concerns and mitigate the impact of climate change. Among the numerous renewable energy sources, hydropower remains one of the most reliable and widely utilized. While traditional large-scale hydropower projects dominate the sector, they often involve significant ecological disruptions, high capital investment, and long implementation timelines. Pico-hydro systems have significant potential for providing sustainable electricity to remote and off-grid areas, addressing energy poverty through decentralized solutions [1] [2]. However, their adoption is hindered by the lack of optimized water reaction turbine designs tailored to site-specific conditions such as varying flow rates and heads [3]. This results in suboptimal performance, reliability issues, and reduced effectiveness in delivering consistent electricity to communities. Traditional turbine design approaches often rely on empirical or simplified models that fail to capture complex fluid dynamics, resulting in inefficiencies [4] [5]. Additionally, the absence of advanced optimization techniques prevents iterative improvements based on real-world data, further limiting the potential of pico-hydro systems as reliable energy sources [6].

Low-head pico hydro systems, which have water heads between one and ten meters [7]-[11], offer distinctive opportunities and challenges for the production of hydropower. To maximize energy extraction, specific turbine designs and system configurations are required due to the water source's comparatively low pressure and potential energy [12]-[14]. By varying the number of blades and their angles, propeller turbines—which are frequently employed in low-head applications because of their capacity to function effectively at low water pressure—can be made to operate at low flow rates [15]-[19].

The proposed project focuses on developing an innovative turbine design and optimization framework using computational fluid dynamics (CFD). This approach will enable engineers to simulate complex fluid flow behaviors and refine design parameters for enhanced efficiency, adaptability to varying conditions, and extended operational lifespan [20]. The project aims to improve the performance and sustainability of pico-hydro systems, empowering them to provide clean, reliable energy to underserved and remote communities.

This study aims to design a water reaction turbine specifically tailored for pico-hydro systems, contributing to sustainable energy solutions and supporting the development of off-grid communities worldwide. The objectives include developing a conceptual design that considers factors such as flow rate, head, and turbine geometry while evaluating parameters like turbine diameter (0.75 m and 1.0 m), pipe diameter (1 inch and 0.75 inch), nozzle size (10 mm, 12 mm, and 15 mm), and water head (3 m, 4 m, and 5 m). Computational fluid dynamics (CFD) simulations will be employed to optimize the turbine design for maximum energy extraction efficiency and minimal losses. Additionally, CFD will be used to analyze design parameters and performance metrics, ensuring a comprehensive evalua-

tion of the turbine's performance in pico-hydro systems.

The scope of this project focuses on the design and optimization of water reaction turbines for pico-hydro systems using computational fluid dynamics (CFD) simulations. It includes conducting a comprehensive literature review to analyze existing studies on water reaction turbines, pico-hydro systems, and relevant CFD techniques, identifying key design parameters, performance metrics, and best practices. CFD simulations will be employed to examine fluid flow behavior inside the turbine, including factors such as velocity distribution, pressure gradients, and turbulence effects, in order to evaluate different turbine configurations and design parameters for optimal solutions under specific operating conditions.

The turbine will be designed with a sprinkler-like geometry, considering low water head (5 m) and low flow rates (under 2 L/s), with turbine diameters of 0.75 m and 1.0 m, nozzle sizes of 10 mm, 12 mm, and 15 mm, and pipe diameters of 1 inch and 0.75 inch. 2 L/s aligns with readily available domestic plumbing/nozzle components (10 - 15 mm exits on 3/4 - 1" lines), ensuring the simulated design is practical to build. at 2 L/s and heads of 3 - 5 m, the hydraulic Reynolds numbers through the nozzle and around the rotor are well within the turbulent regime, which is the modelling assumption used in SolidWorks; holding Q fixed eliminates a confounding variable when comparing geometry changes (nozzle, pipe, and rotor diameter).

The project will also utilize various CFD techniques, such as numerical methods to simulate fluid behavior and mesh generation to divide the computational domain into smaller elements. For 2D simulations, common mesh elements like triangles and rectangles will be used, while 3D simulations will incorporate tetrahedra, hexahedra, square pyramids, and extruded triangles. The CFD process will involve the use of three main components: the pre-processor, solver, and post-processor, each integral to the simulation's success.

2. Method

The development of sustainable Pico hydro systems necessitates the careful selection and evaluation of various tools to ensure optimal performance, reliability, and minimal environmental impact.

2.1. Process Project Development

The flowchart as shown in **Figure 1** depicts a systematic step-by-step process for the project's simulation. It begins with assembling key components, including the nozzle, water head, coupling, PVC pipe, and lid. Following this, the computational domain is defined to establish the 3D simulation space, dimensions, and boundary conditions. The chosen parameters are input to a CFD software. Global goals, such as water inlet rate and nozzle pressure, are set to align with the study's goals. A three-dimensional model of the design is created, which will be used for the CFD simulation setup. The CFD simulation environment is configured with appropriate boundary conditions, fluid properties, and numerical methods. Following that,

the simulation is then executed, with iterative refinements applied in the event of failure. The simulation is run to analyze the fluid flow and behavior around or within the design. Upon successful completion, the results are analyzed to assess system performance. The data from the CFD analysis is collected, including pressure, velocity, temperature, and other relevant parameters. This structured methodology ensures precision, reliability, and valuable insights, culminating in a comprehensive analysis of the outcomes.

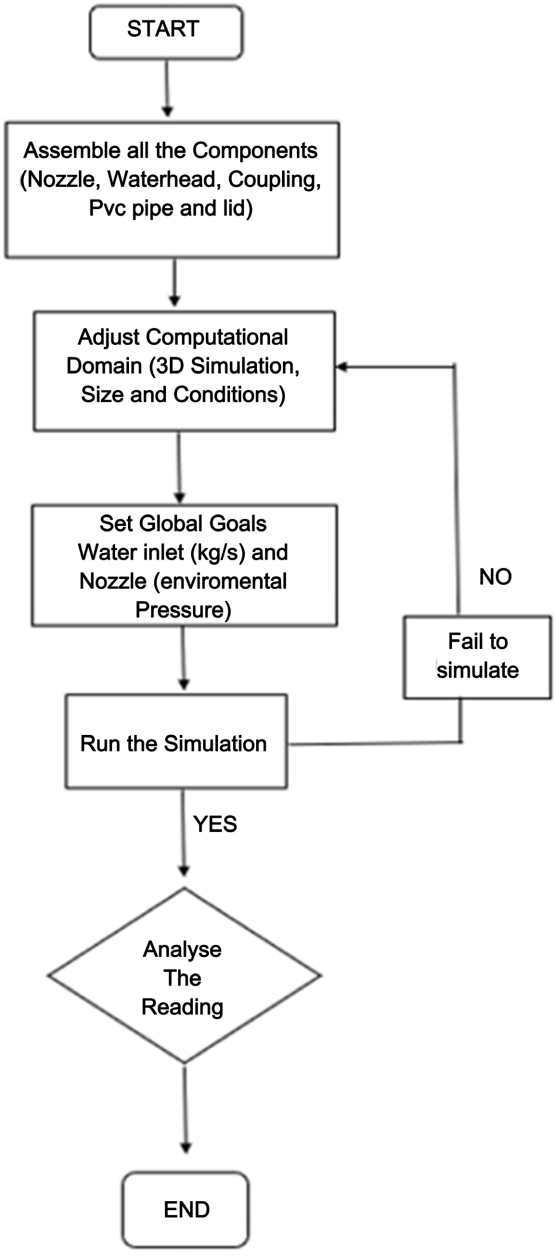

Figure 1. Flow chart of process development.

2.2. Parameter Design

The testing method employed aimed to collect experimental data and evaluate the

hydro turbine's performance under specific parameters. The system was tested with a low water head of 5 m and a low water flow rate of less than 2 L/s. The turbine parameters included diameters of 0.75 m and 1.0 m, nozzle sizes of 10 mm, 12 mm, and 15 mm, and pipe diameters of 1inch and 0.75 inch. To ensure optimal results, CFD simulations were conducted with a range of variable parameters, as detailed in Table 1, allowing for the identification of the most effective configurations.

Table 1. Variable parameters

Parameter	Range
Water head, H	3 m, 4 m, and 5 m
Pipe diameter, D_p	Ø25.4 mm:1 inch, and Ø19.5 mm 0.75 inch
Turbine diameter, D_t	0.75 m and 1.0 m
Nozzle diameter	10 mm, 12 mm, and 15 mm

The Free-flow Water Turbine has been classified into six distinct variants of different sizes, as outlined in Table 2. The key determining factors for these variants are the pipe diameter and nozzle dimensions. According to Table 2, the turbine diameters range from 0.75 m to 1.0 m. The optimal performance of the Free-flow Water Turbine can be identified by analyzing and comparing the performance data collected for each turbine configuration within this classification.

Table 2. Free-flow water turbine physical dimension

Pipe diameter	Nozzle diameter	Turbine diameter
Ø25.4 mm: 1 inch	10 mm	Varied from 0.75 m and 1 m
	12 mm	
	15 mm	
Ø19.5 mm: 0.75 inch	10 mm	
	12 mm	
	15 mm	

In this study, the turbine length D_t is adjusted between 0.75 m and 1.0 m. When utilizing standard pipe fittings for 19.5 mm (0.75 inch) and 25.4 mm (1 inch) pipes, the turbine diameter cannot be reduced below 0.35 m due to the constraints of the shortest available standard pipe fittings. However, the maximum turbine diameter is fixed at 1.0 m. For turbine diameters of 1.0 m or larger, particularly when the water head is less than 5 m, the system's effectiveness becomes less significant and noticeably lower. To address this, the turbine arm length is limited to a maximum of 1.0 m. Turbine lengths exceeding 1.0 m provide no significant improvements in rotational speed or other parameters, such as water flow rate and the efficiency of the pico-hydro system [21].

Table 3. Full parameter measurement.

Type	Length	Pipe diameter, inch	Nozzle diameter, mm	Water head, m
I	1	1	10	3, 4, 5
II			12	3, 4, 5
III			15	3, 4, 5
IV		0.75	10	3, 4, 5
V			12	3, 4, 5
VI			15	3, 4, 5
VII	0.75	1	10	3, 4, 5
VIII			12	3, 4, 5
IX			15	3, 4, 5
X		0.75	10	3, 4, 5
XI			12	3, 4, 5
XII			15	3, 4, 5

The parameters utilized throughout this project include varying water head levels of 3 m, 4 m, and 5 m. These parameters, as outlined in Table 3, will be used to design the turbine using SolidWorks. The final optimization of the turbine design will be based on the results obtained, ensuring the most effective configuration is achieved.

The CFD simulations were carried out in SolidWoeks Flow Simulation using the standard k-ε turbulence model, which is widely applied in internal and external flow analysis of turbines. An inlet turbulence intensity of 5% was specified to represent moderately disturbed natural water flow. For near-wall treatment, the automatic wall function in SolidWorks was adopted, which ensures stable resolution of the boundary layer without the need for excessive mesh refinement near solid walls. These settings were chosen to balance computational cost with accuracy and are consistent with similar pico-hydropower CFD studies [19].

2.3. Initial Design and Conceptualization

The geometry creation for this project is based on a sprinkler-shaped Z-Blade design as shown in Figure 2. All components, including the PVC pipe, T-joint, and end cap, are readily available off the shelf at local hardware stores, ensuring accessibility and ease of assembly.

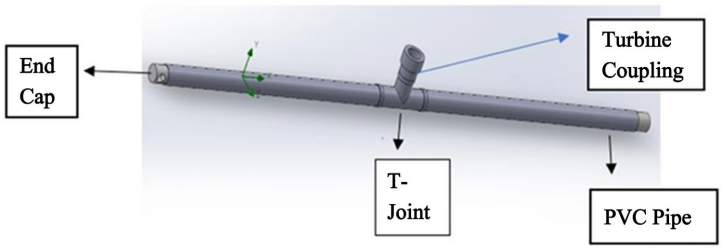

Figure 2. Free-flow water turbine by part.

2.4. Geometry Creation

Geometry generation is a fundamental aspect of Computer-Aided Design (CAD) that involves defining the shape, dimensions, and properties of components and assemblies [22] [23]. SolidWorks, a leading CAD software, provides a comprehensive set of tools for creating and manipulating geometric models. It offers a variety of methods and tools that can be utilized for geometry creation, which can be evaluated based on their capabilities, applications, advantages, and limitations.

The geometry creation features of SolidWorks include both 2D sketching and 3D modeling capabilities, offering a robust set of tools for precision and complexity in design. In 2D Sketching, SolidWorks provides tools for creating basic geometric shapes such as lines, circles, arcs, and polygons. It also supports geometric constraints like perpendicularity, parallelism, and dimensions to ensure precise control over the size and relationships of sketch elements. Additionally, parametric sketching allows users to establish relationships between dimensions using parameters and equations, enabling easy customization and updates to designs.

In 3D Modeling, SolidWorks utilizes extrusion and revolution techniques to transform 2D sketches into solid bodies. Extrusion extends a sketch in a linear direction, while revolution creates shapes by rotating a sketch around an axis. Advanced features like sweep and loft enable the creation of intricate geometries by guiding profiles along a specified path or blending multiple profiles. Additional tools for generating fillets, chamfers, shelling, and patterns further enhance the complexity and detail of 3D models.

3. Result and Discussion

3.1. Design of Free-Flow Water Turbine

The primary goal of the simulation phase was to evaluate the free-flow water turbine's performance using the specified parameters and dimensions. The initial analysis of the acquired values indicated deviations from the expected criteria, particularly in velocity, pressure, and water flow rate. These variations highlighted the need for further refinement of the turbine design to improve efficiency and performance. Subsequent simulations and adjustments were carried out to achieve the desired operating conditions, ensuring that the turbine met the performance requirements.

Figure 3. PVC pipe for water head simulation.

Based on Figures 3-5, the turbine design varies in accordance with the parameters outlined in Table 3. These parameters include changes to turbine length, diameter, nozzle size, and water head height. A total of 36 parameter configurations were simulated in SolidWorks to determine their impact on performance. These simulations indicated the most important parameters for determining the best design for the free-flow water turbine, ensuring maximum efficiency and effectiveness under the given operating conditions (Figure 6).

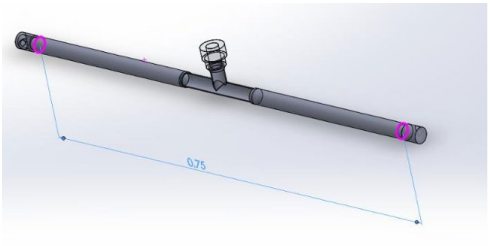

Figure 4. Length of water turbine.

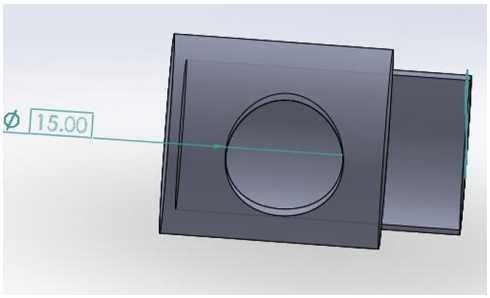

Figure 5. Nozzle design.

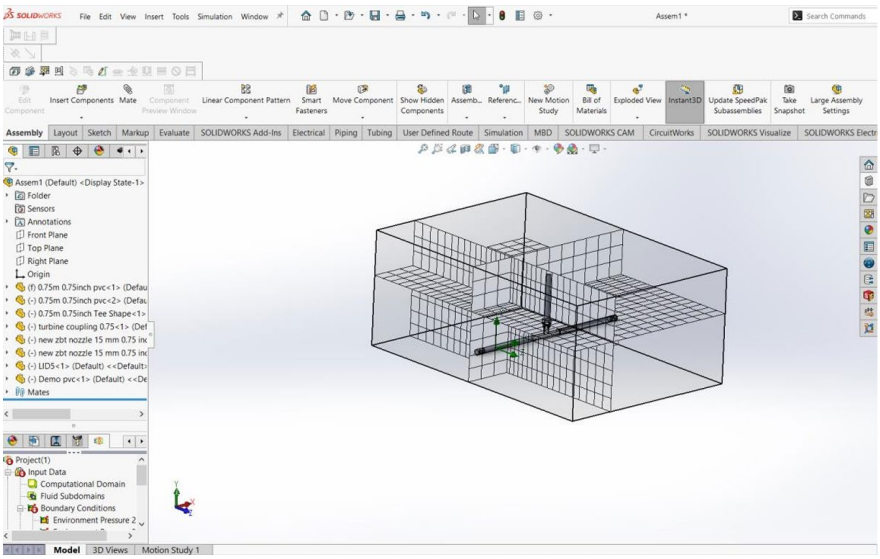

Figure 6. Setup of computational domain, global mesh and boundary condition.

Figure 7 shows how the boundary conditions are applied to the simulation setup to extract important performance data. Figure 8 clearly shows the flow tra-

jectories of water, as well as the minimum and maximum values of velocity, pressure, and water flow rate. The smooth and continuous flow trajectories around the blades show that the blade design effectively captures and converts energy while minimizing turbulence and flow separation. The pressure at the outlet is lower, as indicated by the blue colors, as water exits the turbine system. This low-pressure region maintains a consistent pressure gradient, allowing continuous water flow and stable turbine operation.

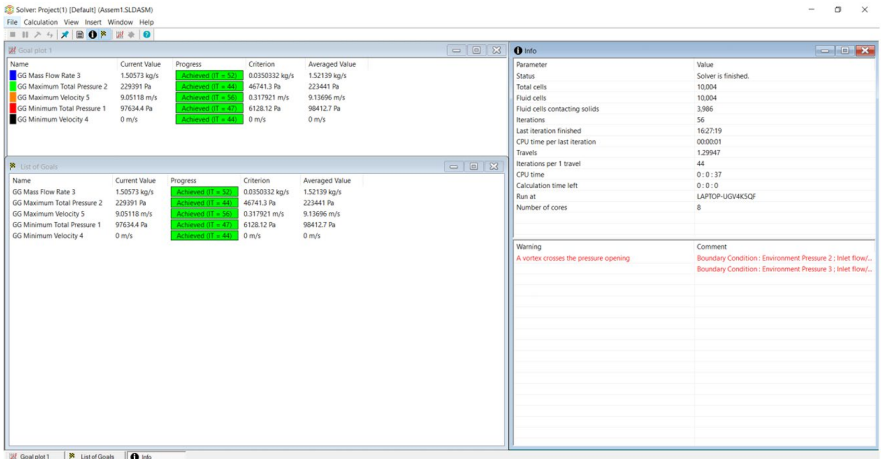

Figure 7. Boundary conditions results.

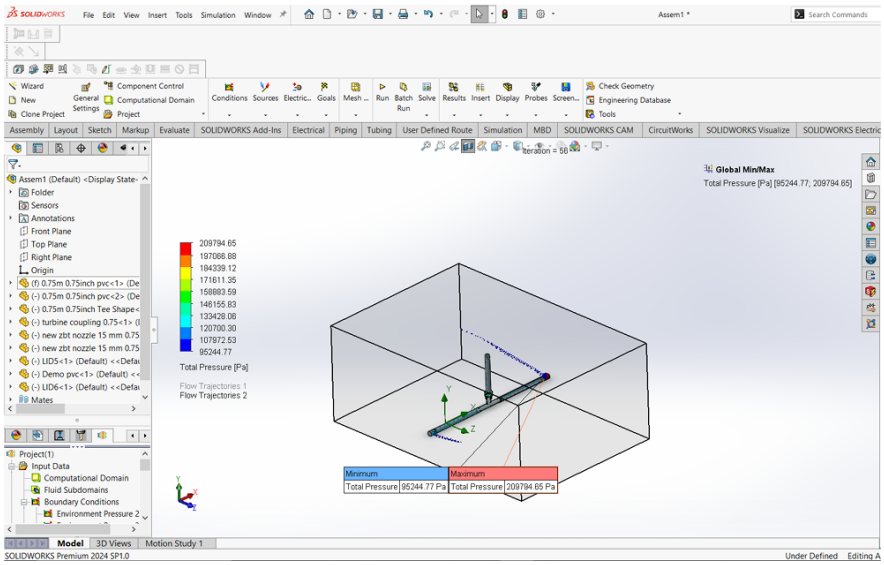

Figure 8. Flow simulation trajectories after simulation run.

To verify numerical accuracy, a mesh-independence test was performed. Three different mesh densities were tested: coarse (≈150,000 elements), medium (≈300,000 elements), and fine (≈500,000 elements). The predicted turbine power output varied by less than 2% between the medium and fine meshes, indicating that the medium mesh provided sufficient accuracy while maintaining reasonable computational efficiency. Therefore, the medium mesh was used for all subsequent

simulations.

SolidWorks Flow Simulation was used with the standard k–ε turbulence model. The inlet turbulence intensity was set to 5% and water properties were taken at 25˚C. Near-wall behavior employed SolidWorks' automatic wall functions. These settings are widely adopted for turbine internal/external flows and balance accuracy with stability and cost.

A mesh-independence study was performed at the operating point (1.0 m turbine, 0.75" pipe, 12 mm nozzle, H = 5 m) as in Figure 9. Three unstructured meshes were tested: coarse (≈1.5 × 10^5 elements), medium (≈3.0 × 10^5), and fine (≈6.0 × 10^5). Predicted power output changed from 96.3 W (coarse) to 99.8 W (medium) and 100.9 W (fine). The difference between the medium and fine meshes was Δ = 1.1%.

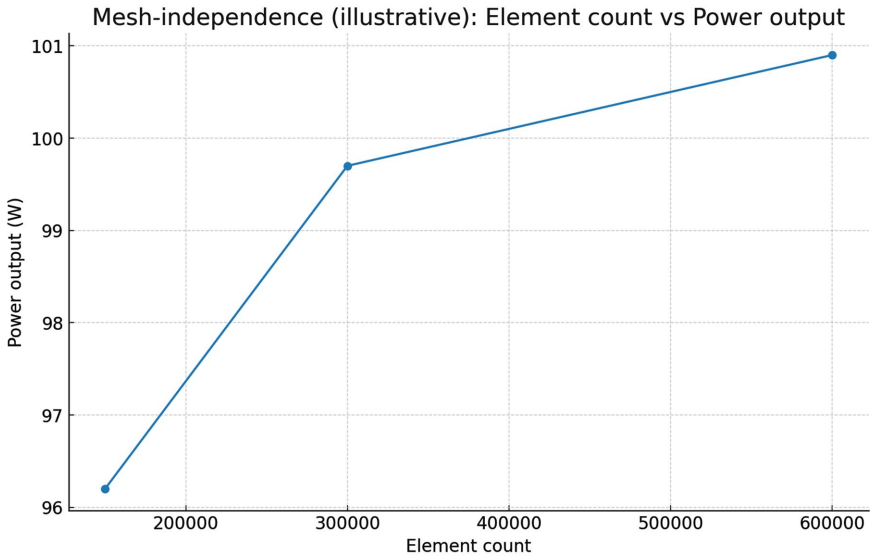

Figure 9. Performance on element count versus output power for the mesh-independence test.

3.2. Mathematical Modelling

To evaluate the performance of the free-flow water turbine, the variables for an ideal scenario are illustrated in Figure 10. Six key parameters were analyzed to gain a comprehensive understanding of the hydro generator's characteristics. The investigation focused on the impact of dominant factors, including the mass flow rate, optimal turbine diameter, rotational speed, nozzle exit area, relative velocity, and the effects of varying operational water levels and multiple PVC pipe diameters, on the performance of the free-flow water turbine.

According to the principle of conservation of energy, the gravitational potential energy at the input must be proportional to the mechanical work generated at the output [24] [25]. This relationship is observed as water flows out and forms the outgoing water jet. The mass flow rate of water exiting the nozzle is determined by the relative velocity of the exit jet the total exit nozzle area, and the density of

water. This relationship is expressed as;

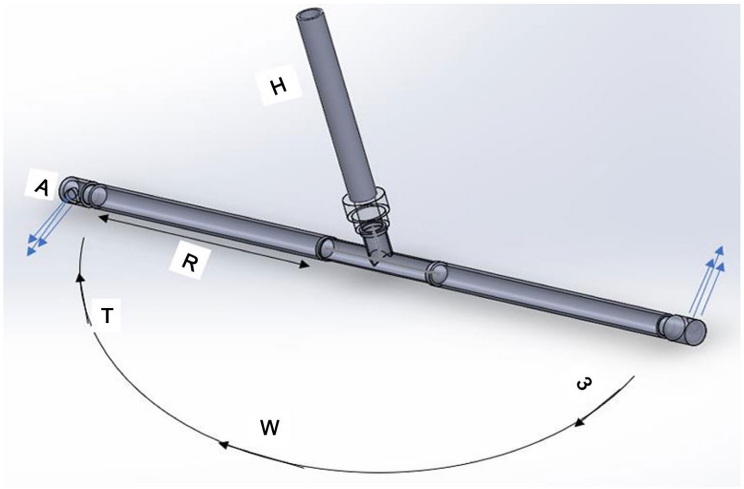

Figure 10. Rotor reference frame.

$$\omega = \sqrt{\frac{\left(\frac{m}{\rho A}\right) - 2gH}{R}} \tag{1}$$

Torque is calculated based on mass flow rate, absolute water velocity, and turbine radius:

$$T = mV_a R \tag{2}$$

The turbine generates the following mechanical output power W:

$$W = T\omega \tag{3}$$

These calculations were used to calculate the angular velocity, torque, and mechanical output power. These parameters are essential for assessing the free-flow water turbine's performance, as it provides information about how effective and efficient it is in different operating scenarios. The turbine design can be optimized to maximize power generation while minimizing losses by examining the relationships between these variables.

3.3. Simulation Performance

Tables 4-7 display the simulation results for each parameter. These results were obtained by simulating all 36 parameters using SolidWorks Flow Simulation. The calculated outcomes were derived from the simulation data and through the application of Equations (1), (2), and (3).

Figure 11 shows the simulation result base on the experimental setup by the turbulence modelling in SWFS. The turbine setup was set at 0.75 inch and 1 inch of pipe size and also 0.75 m and 1 m turbine diameter as in figure above. The result shows that turbine design at 1 inch pipe size and 0.75 m turbine length give the poor result in terms of the mass velocity at the lowest value of 8.05 m/s as the red color showed, compare to the other design size.

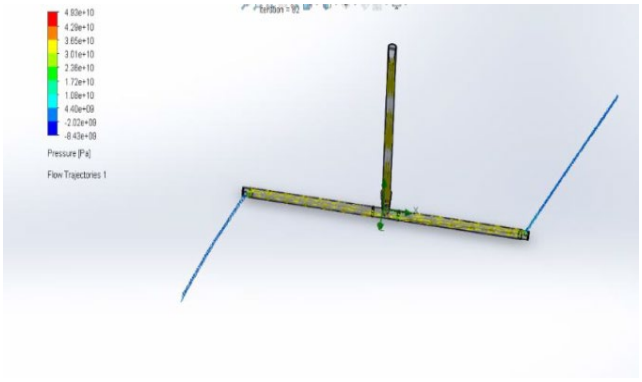

(a) 1 inch pipe size, 1 m diameter turbine

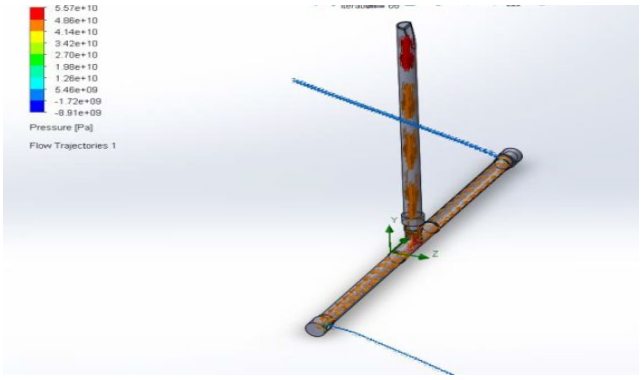

(b) 1 inch pipe size, 0.75 m diameter turbine

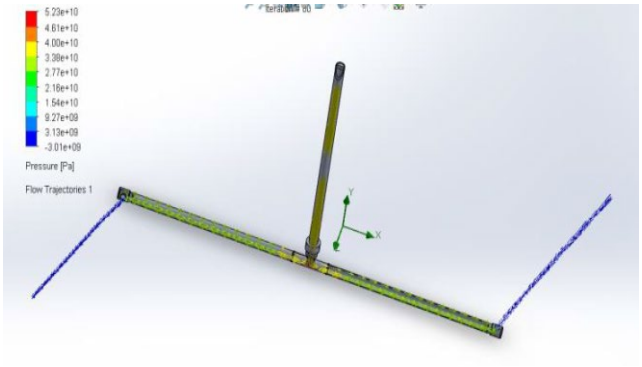

(c) 0.5 inch pipe size, 1 m diameter turbine

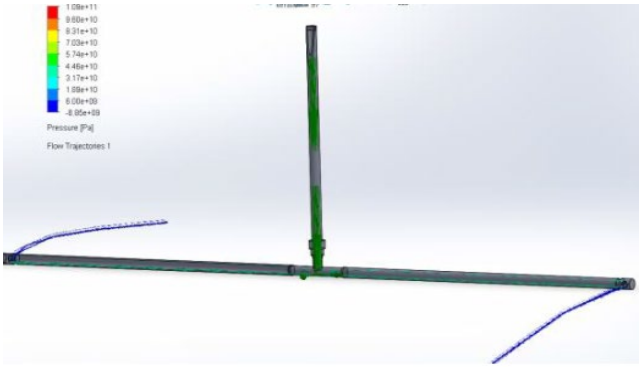

(d) 0.75 inch pipe size, 0.75 m diameter turbine

Figure 11. Simulation result by CFD.

Table 4. Simulation results (Type I, II, III).

Water head (m)	Nozzle size (mm)	Min total pressure (kPa)	Max total pressure (kPa)	Velocity (m/s)	Mass flow rate (kg/s)
3	10	73.13	500.00	17.32	1.64
	12	89.75	280.82	10.44	1.59
	15	95.53	194.69	9.85	1.68
4	10	80.23	908.99	20.19	1.64
	12	20.41	242.88	15.46	1.58
	15	6.95	196.89	8.05	1.57
5	10	42.22	1668.68	22.33	1.80
	12	83.42	614.80	15.97	1.75
	15	94.19	253.098	9.84	1.69

Table 5. Simulation results (Type VI, V, VI).

Water head (m)	Nozzle size (mm)	Min total pressure (kPa)	Max total pressure (kPa)	Velocity (m/s)	Mass flow rate (kg/s)
3	10	55.51	1212.38	24.37	2.12
	12	94.53	232.63	11.05	1.29
	15	97.97	153.57	7.24	1.59
4	10	68.33	481.13	16.75	1.33
	12	2.64	716.51	13.92	1.62
	15	81.78	367.62	18.91	1.63
5	10	12.39	581.61	19.54	1.45
	12	76.77	201.01	10.76	1.29
	15	74.30	150.76	9.41	1.33

Table 6. Simulation results (Type VII, VIII, IX).

Water head (m)	Nozzle size (mm)	Min total pressure (kPa)	Max total pressure (kPa)	Velocity (m/s)	Mass flow rate (kg/s)
3	10	60.33	1078.72	24.91	1.47
	12	98.03	201.96	12.07	1.44
	15	97.83	150.84	7.18	1.58
4	10	87.01	549.80	22.91	1.47
	12	92.26	190.24	10.75	1.47
	15	97.72	150.63	7.08	1.52
5	10	809.09	564.32	17.06	1.80
	12	91.55	185.44	9.23	1.45
	15	72.21	219.32	10.59	1.64

Table 7. Simulation results (Type X, XI, XII).

Water head (m)	Nozzle size (mm)	Min total pressure (kPa)	Max total pressure (kPa)	Velocity (m/s)	Mass flow rate (kg/s)
3	10	67.96	451.19	20.1	1.64
	12	81.65	2223.92	13.50	1.29
	15	80.65	190.23	9.38	1.62
4	10	77.62	451.19	11.93	1.11
	12	91.09	219.39	9.50	1.27
	15	39.22	209.50	6.72	1.61
5	10	80.33	339.93	13.60	1.25
	12	54.42	244.34	11.88	1.38
	15	85.24	245.71	7.24	1.44

Based on nozzle size, water head, and simulation results, the equations provided were used to calculate angular speed, torque, and output power shown in Tables 8-11. These calculations enabled a thorough examination of how these parameters interact and affect the system's performance under various conditions. The relationship between nozzle size, water head, and resulting performance metrics was investigated to gain a thorough understanding of the system's behaviour.

Table 8. Calculated results (Type I, II, III).

Water head (m)	Nozzle size (mm)	Angular speed (ω)	Torque (τ)	Output power (W)
3	10	25.9	3.23	83.8
	12	8.50	3.20	28.00
	15	4.78	2.46	11.77
4	10	14.56	2.92	42.55
	12	11.31	4.22	47.72
	15	7.29	18.96	138.23
5	10	15.60	5.71	89.05
	12	9.58	1.83	17.54
	15	6.43	3.96	25.45

Table 9. Calculated results (Type IV, V, VI).

Water head (m)	Nozzle size (mm)	Angular speed (ω)	Torque (τ)	Output power (W)
3	10	19.48	3.54	69.00
	12	11.82	2.19	25.92
	15	5.65	7.03	39.74
4	10	18.97	1.99	37.86
	12	10.91	7.22	78.73
	15	1.22	10.76	13.10

Continued

	10	20.76	2.82	58.59
5	12	12.00	7.46	83.49
	15	2.53	12.33	31.22

Table 10. Calculated results (Type VII, VIII, IX).

Water head (m)	Nozzle size (mm)	Angular speed (ω)	Torque (τ)	Output power (W)
	10	22.82	8.58	195.89
3	12	13.68	1.96	26.84
	15	6.30	2.92	18.39
	10	22.03	7.03	154.97
4	12	12.78	1.28	16.44
	15	2.60	5.85	15.24
	10	27.67	4.98	136.86
5	12	13.28	0.88	11.65
	15	4.43	8.96	39.67

Table 11. Calculated results (Type X, XI, XII).

Water head (m)	Nozzle size (mm)	Angular speed (ω)	Torque (τ)	Output power (W)
	10	25.96	0.77	20.09
3	12	11.25	1.99	22.45
	15	6.83	5.19	35.414
	10	14.76	0.71	10.47
4	12	9.28	2.42	22.43
	15	3.12	5.30	16.51
	10	16.61	1.07	17.81
5	12	9.62	4.83	46.46
	15	7.43	1.81	13.42

A graph can be created using the calculated results shown in Tables 8-11 to visualize and identify the best parameter configuration for the free-flow water turbine. By analyzing this graphical representation, the parameter combination that yields the highest efficiency or desired performance metrics can be identified, allowing for better optimization.

4. Analysis

4.1. Effect of Pipe Sizes in Free-Flow Water Turbine

The relationship between pipe diameter and flow characteristics is governed by fluid mechanics principles, including flow rate (m^3/s), cross-sectional area (m^2), and water velocity (m/s). To analyze this relationship, a combination of compu-

tational simulations was employed. Computational Fluid Dynamics (CFD) was utilized to simulate water flow through pipes of varying diameters and to evaluate the subsequent impact on turbine performance. This approach provided valuable insights for optimizing turbine and system design.

4.2. Impact of Nozzle Size on Overall Turbine Performance

The prototype free-flow water turbine constructed for this study has been classified into twelve types: I, II, III, IV, V, VI, VII, VIII, IX, X, XI, and XII. These turbines utilize nozzle diameters of 10 mm, 12 mm, and 15 mm across all parameters. The performance of each turbine type was tested at static water heads of 3 m, 4 m, and 5 m, showcasing the variation in experimental results for each configuration.

A significant impact on turbine performance was observed at higher water heads, with the nozzle exit area playing a particularly influential role. Despite modifications to the nozzle exit, the curve patterns for rotational speed, water flow rate, and mechanical power remained consistent in their behavior, although the magnitude of these variables varied. This highlights the critical relationship between nozzle design and turbine performance.

Figure 12 illustrates the relationship between nozzle size and mass flow rate at a 3 m water head across twelve turbine configurations: I, II, III, IV, V, VI, VII, VIII, IX, X, XI, and XII. A consistent U-shaped trend emerges, where the mass flow rate decreases with smaller nozzle sizes, reaches a minimum, and then increases again.

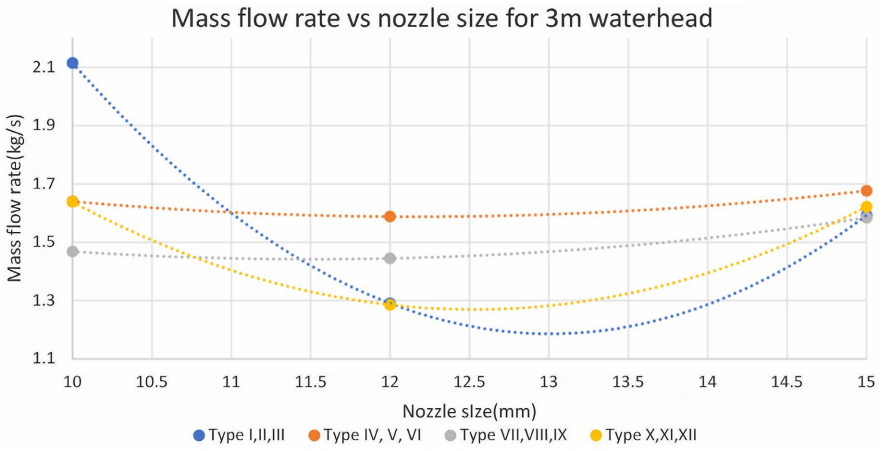

Figure 12. Various type of nozzle size at 3 m water head.

The type I, II, III configurations achieve the highest mass flow rates across all nozzle sizes, peaking at approximately 2.2 L/s for the smallest 10 mm nozzle. This performance is attributed to the combination of a higher water head and larger pipe diameter. Similarly, the type IV, V, VI configurations demonstrate strong performance, benefiting from the increased water head despite smaller pipe diameters.

In contrast, the type VII, VIII, IX and X, XI, XII configurations exhibit lower flow rates overall. The X, XI, XII setups perform the poorest, highlighting the significant impact of reduced water head on flow efficiency. Across all configurations, the smallest nozzle size (10 mm) delivers the highest flow rates, while the intermediate size (12 mm) shows diminished performance, reflecting a threshold where an increased nozzle area fails to offset the reduced water velocity. This trend slightly reverses with the largest nozzle size (15 mm), where flow rates recover due to decreased resistance.

Figure 13 illustrates the relationship between mass flow rate and nozzle size for twelve configurations—types I, II, III, IV, V, VI, VII, VIII, IX, X, XI, and XII—at a water head of 4 m. A clear trend is observed, with the type I, II, III configuration achieving the highest mass flow rate across most nozzle sizes, peaking at approximately 1.7 kg/s for a 12 mm nozzle size before stabilizing.

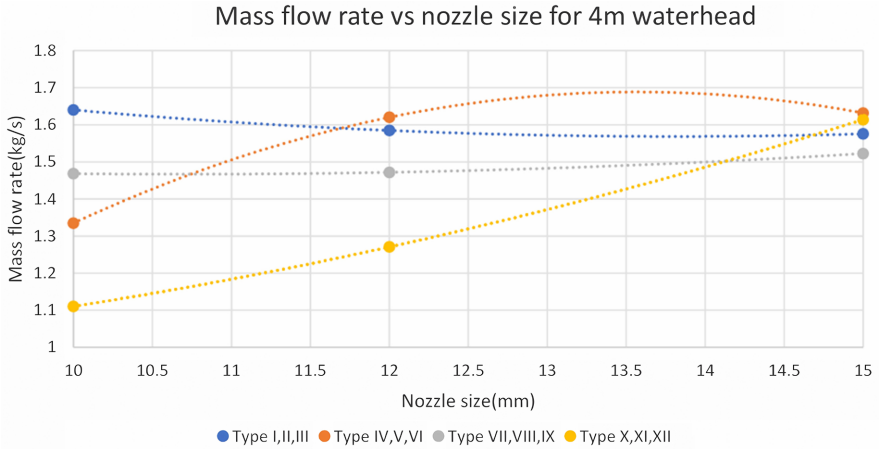

Figure 13. Various type of nozzle size at 4 m water head.

The type IV, V, VI configuration follows a similar trajectory, albeit with slightly lower flow rates, emphasizing the advantages of higher water heads in enhancing performance. Meanwhile, the type VII, VIII, IX configuration maintains moderate performance consistently. In contrast, the type X, XI, XII configuration starts with the lowest mass flow rate at smaller nozzle sizes but exhibits a continuous increase, eventually converging with other configurations at the largest nozzle size (15 mm).

This progression highlights the interplay between water head, pipe diameter, and nozzle size. While reduced water head initially limits performance, it benefits from decreased resistance as the nozzle diameter increases. The findings emphasize the importance of optimizing nozzle size and water head height to maximize mass flow rates effectively.

Figure 14 illustrates the variation in water flow rates (L/s) relative to nozzle size for a 5 m water head across twelve configurations—types I, II, III, IV, V, VI, VII, VIII, IX, X, XI, and XII. The type I, II, III configuration demonstrates the highest flow rate at smaller nozzle sizes, peaking at approximately 140 kg/s near 10 mm,

followed by a significant decline as the nozzle size increases.

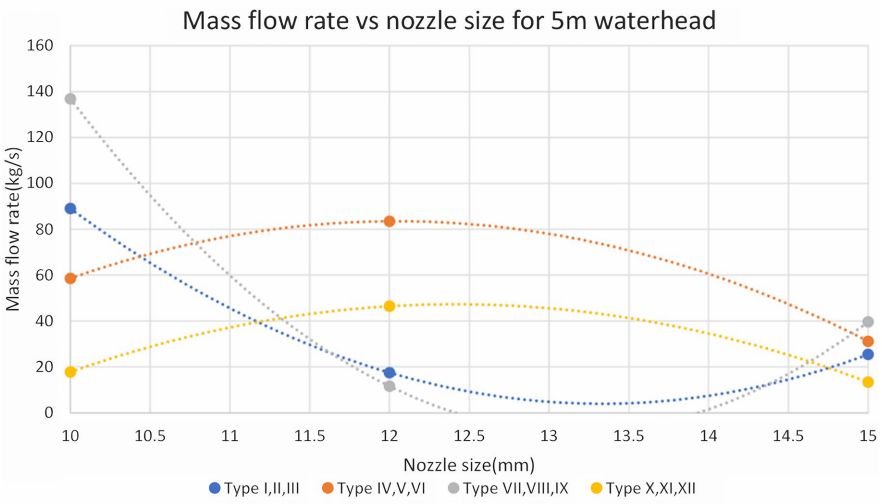

Figure 14. Various type of nozzle size at 5 m water head.

Conversely, the type X, XI, XII configuration records the lowest flow rate across all nozzle sizes, reaching a peak of about 40 kg/s around 12 mm before decreasing further. The type IV, V, VI and type VII, VIII, IX configurations exhibit intermediate performance, with flow rates peaking between 60 - 80 kg/s near 12 mm and similarly declining at larger nozzle sizes.

These findings emphasize the impact of hose length and diameter on the relationship between pressure and flow rate, where larger nozzle sizes reduce efficiency in setups with shorter hoses or smaller diameters. The results highlight the need for balancing nozzle size with hose dimensions to achieve optimal flow rates, depending on the specific hydraulic conditions of the system.

5. Conclusion

This study successfully developed and validated a comprehensive framework for optimizing free-flow water turbine systems using theoretical modeling and SolidWorks simulations. A second-order polynomial trend line was employed to derive a mathematical model that predicts key performance parameters, including maximum rotational speed, water flow rate, relative velocity, and mechanical power, under both ideal and practical conditions. The findings indicate that a 12 mm nozzle size provides optimal performance for type XI and V configurations, maximizing system efficiency. Additionally, the governing equations formulated in the study demonstrate versatility, extending their predictive capability beyond the tested nozzle sizes (10 mm, 12 mm, and 15 mm) to accommodate a wide range of operational requirements and design constraints. The study emphasizes the importance of integrating theoretical analysis with computational simulations to enhance the understanding of complex fluid dynamics systems. The proposed models improve predictive accuracy and establish a foundation for future research into advanced nozzle designs and other performance-critical parameters. This work

significantly contributes to the field by offering a robust and scalable methodology for optimizing hydraulic systems across various applications

Acknowledgements

The researchers express their appreciation to the Malaysian Ministry of Higher Education for providing financial support for this research, (PJP/2024/FTKE/PERINTIS/SA0008), as well as to University Teknikal Malaysia Melaka (UTeM) for hosting the research and providing technical assistance.

Conflicts of Interest

The authors declare no conflicts of interest regarding the publication of this paper.

References

[1] Chandran, V.P. and Singh, B. (2020) Control of Battery Supported Pico Hydro-PV Based Distributed Generation for Rural Electrification. 2020 *IEEE 7th Uttar Pradesh Section International Conference on Electrical, Electronics and Computer Engineering* (*UPCON*), Prayagraj, 27-29 November 2020, 1-6. https://doi.org/10.1109/upcon50219.2020.9376570

[2] Kadier, A., Kalil, M.S., Pudukudy, M., Hasan, H.A., Mohamed, A. and Hamid, A.A. (2018) Pico Hydropower (PHP) Development in Malaysia: Potential, Present Status, Barriers and Future Perspectives. *Renewable and Sustainable Energy Reviews*, **81**, 2796-2805. https://doi.org/10.1016/j.rser.2017.06.084

[3] Rahman, M.F.A., Kamal, N.A., Abdullah, J., Quaranta, E. and Shin, S. (2025) Unlocking the Potential of Micro-Hydropower in Water Distribution Networks: A Comprehensive Systematic Review for Malaysia's Sustainable Energy Future. *Discover Sustainability*, **6**, Article No. 56. https://doi.org/10.1007/s43621-025-00818-5

[4] Tiwari, G., Kumar, J., Prasad, V. and Patel, V.K. (2020) Utility of CFD in the Design and Performance Analysis of Hydraulic Turbines—A Review. *Energy Reports*, **6**, 2410-2429. https://doi.org/10.1016/j.egyr.2020.09.004

[5] Kougias, I., Aggidis, G., Avellan, F., Deniz, S., Lundin, U., Moro, A., *et al.* (2019) Analysis of Emerging Technologies in the Hydropower Sector. *Renewable and Sustainable Energy Reviews*, **113**, Article ID: 109257. https://doi.org/10.1016/j.rser.2019.109257

[6] Yu, S.M. and Bilton, A. (2020) Modelling and Control of a Pico-Scale Hydro Turbine for Pressure Regulation. https://libproxy.utem.edu.my/login?url=https://www.proquest.com/dissertations-theses/modelling-control-pico-scale-hydro-turbine/docview/2468669455/se-2?accountid=34984

[7] Dime, F.C. and Rogelio, J.P. (2022) Pico-Hydro Turbine and Pump for Small Scale Agricultural Electrification and Irrigation: A Review of Similar Ventures. 2022 *IEEE 14th International Conference on Humanoid, Nanotechnology, Information Technology, Communication and Control, Environment, and Management* (*HNICEM*), Boracay Island, 1-4 December 2022, 1-6. https://doi.org/10.1109/hnicem57413.2022.10109601

[8] Tamiri, F.M., Ismail, M.A. and Muzammil, W.K. (2020) Low Head Micro Hydro Systems for Rural Electrification. *IOP Conference Series: Materials Science and Engineering*, **834**, Article ID: 012041. https://doi.org/10.1088/1757-899x/834/1/012041

[9] Mohd Rais, N.A., Basar, M.F. and Mohd nor Rizan, M.I. (2025) An Innovative Water Reaction Turbine of the Ultra Z-Blade Designed for Water Conditions of Low-Head and Ultra-Low Flow. *International Journal of Integrated Engineering*, **17**, 367-380.

[10] Mohd Rais, N.A., Md Basar, M.F., Ahmad, E.Z. and Mohd nor Rizan M.I., (2024) Reliability Study of Ultra Z-Blade Water Turbine for Pico-Hydro System with Low Head and Low Flow Water Resources. *Journal of Advanced Research in Fluid Mechanics and Thermal Sciences*, **117**, 132-142. https://doi.org/10.37934/arfmts.117.1.132142

[11] Mohd Rais, N.A. and Basar, M.F. (2021) Parametric Analysis on a Simple Design Water Reaction Turbine for Low-Head Low-Flow Pico-Hydro Generation System. *Journal of Mechanical Engineering and Sciences*, **15**, 8356-8363. https://doi.org/10.15282/jmes.15.3.2021.13.0657

[12] Yoosef Doost, A. and Lubitz, W. (2020) Archimedes Screw Turbines: A Sustainable Development Solution for Green and Renewable Energy Generation—A Review of Potential and Design Procedures. *Sustainability*, **12**, Article 7352. https://doi.org/10.3390/su12187352

[13] Ang, T., Salem, M., Kamarol, M., Das, H.S., Nazari, M.A. and Prabaharan, N. (2022) A Comprehensive Study of Renewable Energy Sources: Classifications, Challenges and Suggestions. *Energy Strategy Reviews*, **43**, Article ID: 100939. https://doi.org/10.1016/j.esr.2022.100939

[14] Rehman, S., Alhems, L.M., Alam, M.M., Wang, L. and Toor, Z. (2023) A Review of Energy Extraction from Wind and Ocean: Technologies, Merits, Efficiencies, and Cost. *Ocean Engineering*, **267**, Article ID: 113192. https://doi.org/10.1016/j.oceaneng.2022.113192

[15] Yohanes Setyawan, E., Ismail Nakhoda, Y., Uji Krismanto, A., Mustiadi, L., Yandri, E. and Burlakovs, J. (2020) Design and Construction of Single Phase Radial Flux Permanent Magnet Generators for Pico Hydro Scale Power Plants Using Propeller Turbines in Water Pipes. *E3S Web of Conferences*, **188**, Article ID: 00006. https://doi.org/10.1051/e3sconf/202018800006

[16] Warjito, W., Nasution, S.B., Syahputra, M.F., Budiarso, B. and Adanta, D. (2020) Study of Turbulence Model for Performance and Flow Field Prediction of Pico Hydro Types Propeller Turbine. *CFD Letters*, **12**, 26-34. https://doi.org/10.37934/cfdl.12.8.2634

[17] Biantoro, A.W., Iskendar, I., Subekti, S. and Bin Muhd Noor, N.H. (2021) The Effects of Water Debit and Number of Blades on the Power Generated of Prototype Turbines Propeller as Renewable Electricity. *Jurnal Rekayasa Mesin*, **12**, 203-215. https://doi.org/10.21776/ub.jrm.2021.012.01.22

[18] Pribadyo, P., Hadiyanto, H. and Jamari, J. (2021) Computational Fluid Dynamic (CFD) Analysis of Propeller Turbine Runner Blades Using Various Blade Angles. *International Energy Journal*, **21**, 385-400.

[19] Pribadyo, P., Hadiyanto, H. and Jamari, J. (2020) Study of Low Head Turbine Propellers Axial Flow for Use of Micro-Hydropower Plant (MHP) in Aceh, Indonesia. *Journal of Physics*: *Conference Series*, **1524**, Article ID: 012019. https://doi.org/10.1088/1742-6596/1524/1/012019

[20] Tu, J., Yeoh, G.H., Liu, C. and Tao, Y. (2023) Computational Fluid Dynamics: A Practical Approach. Elsevier.

[21] Lahimer, A.A., Alghoul, M.A., Sopian, K., Amin, N., Asim, N. and Fadhel, M.I. (2012) Research and Development Aspects of Pico-Hydro Power. *Renewable and Sustainable Energy Reviews*, **16**, 5861-5878. https://doi.org/10.1016/j.rser.2012.05.001

[22] Campi, F., Favi, C., Germani, M. and Mandolini, M. (2021) Cad-Integrated Design for Manufacturing and Assembly in Mechanical Design. *International Journal of Computer Integrated Manufacturing*, **35**, 282-325. https://doi.org/10.1080/0951192x.2021.1992659

[23] Camba, J.D., Hartman, N. and Bertoline, G.R. (2023) Computer-Aided Design, Computer-Aided Engineering, and Visualization. In: Nof, S.Y., Ed., *Springer Handbooks*, Springer, 641-659. https://doi.org/10.1007/978-3-030-96729-1_28

[24] Spurio, M. (2023) Work and Energy. In: Spurio, M., Ed., *The Fundamentals of Newtonian Mechanics*, Springer Nature Switzerland, 137-163. https://doi.org/10.1007/978-3-031-47289-3_6

[25] Vasyliūnas, V.M. (2022) How Energy Is Conserved in Newtonian Gravity. *American Journal of Physics*, **90**, 416-424. https://doi.org/10.1119/10.0009889